J|A|C|S
ARTICLES
Published on Web 04/21/2006

A Pirouette on a Metallofullerene Sphere: Interconversion of Isomers of *N*-Tritylpyrrolidino I_h $Sc_3N@C_{80}$

Ting Cai, Carla Slebodnick, Liaosa Xu, Kim Harich, Thomas E. Glass, Christopher Chancellor,‡ James C. Fettinger,‡ Marilyn M. Olmstead,‡ Alan L. Balch,‡ Harry W. Gibson,* and Harry C. Dorn*

Contribution from the Department of Chemistry, Virginia Polytechnic Institute and State University, Blacksburg, Virginia, 24060-0212, and Department of Chemistry, University of California, Davis, California 95616

Received January 20, 2006; E-mail: hdorn@vt.edu; hwgibson@vt.edu

Abstract: The pure I_h isomer of $Sc_3N@C_{80}$ was allowed to react with *N*-triphenylmethyl-5-oxazolidinone via the corresponding azomethine ylide. The reaction results in the formation of two monoadducts; one (**1b**) is the kinetic product, and the other (**1a**) is thermodynamically more stable. Small amounts of the bisadducts were also formed. The structure of the thermodynamic monoadduct **1a** was shown conclusively by NMR spectroscopy and X-ray crystallography to result from addition across the 5,6-ring junction. The kinetic product **1b** was demonstrated to be the 6,6-ring juncture adduct on the basis of NMR experiments and X-ray crystallography. In refluxing chlorobenzene pure **1b** was converted to the more thermodynamically stable **1a** isomer. These *N*-tritylpyrrolidino derivatives are potentially useful precursor compounds for further derivatization for various applications.

Introduction

Endohedral metallofullerenes (EMFs) are novel molecules that encapsulate metal atoms in carbon cages. Because of their unique structures, various potential applications have been proposed since their discovery.[1] In particular, trimetallic nitride template TNT EMFs ($A_3N@C_{80}$, A = lanthanide atom)[2] are some of the most promising fullerene-based materials (e.g., MRI and X-ray contrast agents[3]) because of their high yields compared to classic endohedral metallofullerenes. Theoretical calculations demonstrate that the TNT EMFs are stabilized by six electrons transferred from the trimetallic nitride (A_3N) cluster to the C_{80} cage, resulting in a closed shell electronic structure described as $A_3N^{6+}@C_{80}^{6-}$.[4] Based on the extraordinarily high stabilities of TNT EMFs relative to those of empty cage fullerenes and classic endohedral metallofullerenes,[5,6] macroscopic quantities of high-purity TNT EMFs were recently obtained directly from crude soots in a single facile step by using a cyclopentadiene-functionalized resin to trap the more reactive species via Diels−Alder reactions, allowing the TNT EMFs to pass through.[7]

On the basis of the reaction of C_{60} reported by Prato et al.,[8] we recently synthesized and isolated the first *N*-methylpyrrolidino derivatives of both diamagnetic and paramagnetic TNT EMFs via 1,3-dipolar cycloaddition of azomethine ylides.[9] The demonstration of planar symmetry in the *N*-methylpyrrolidino derivatives by ^{13}C NMR spectroscopy suggested that the reaction took place at the 5,6-ring junction, as we observed earlier for an isochromanone Diels−Alder adduct.[10] Echegoyen et al. reported selective 5,6-ring junction cycloaddition of *N*-ethylazomethine ylide to I_h symmetrical $Sc_3N@C_{80}$.[11] Echegoyen et al. also reported the impact of changing the metal of the internal cluster from Sc to Y; the cycloaddition of *N*-ethylazomethine ylide to $Y_3N@C_{80}$ was reported to occur exclusively at the 6,6-ring junction of the I_h symmetrical C_{80} cage.[12] The thermal retro-

‡ University of California, Davis.

(1) (a) Kobayashi, K.; Nagase, S. In *Endofullerenes: A New Family of Carbon Clusters*; Akasaka, T., Nagase, S., Eds.; Kluwer Academic Publishers: Dordrecht, The Netherlands, 2002; pp 99−119. (b) Shinohara, H. *Rep. Prog. Phys.* **2000**, *63*, 843−892.
(2) Stevenson, S.; Rice, G.; Glass, T.; Harich, K.; Cromer, F.; Jordan, M. R.; Craft, J.; Hadju, E.; Bible, R.; Olmstead, M. M.; Maltra, K.; Fisher, A. J.; Balch, A. L.; Dorn, H. C. *Nature* **1999**, *401*, 55−57.
(3) (a) Iezzi, E. B.; Duchamp, J. C.; Fletcher, K. R.; Glass, T. E.; Dorn, H. C. *Nano Lett.* **2002**, *2*, 1187−1190. (b) Stevenson, S.; Lee, H. M.; Olmstead, M. M.; Kozikowski, C.; Stevenson, P.; Balch, A. L. *Chem. Eur. J.* **2002**, *8*, 4528−4535. (c) Fatouros, P. P.; Corwin, F. D.; Chen, Z.-J.; Broaddus, W. C.; Tatum, J. L.; Ge, Z.; Gibson, H. W.; Kile, J. L.; Leonard, A. P.; Duchamp, J. C.; Dorn, H. C. *Radiology* **2005**, *236*, in press.
(4) (a) Olmstead, M. M.; de Bettencourt-Dias, A.; Duchamp, J. C.; Stevenson, S.; Marciu, D.; Dorn, H. C.; Balch, A. L. *Angew. Chem., Int. Ed.* **2001**, *40*, 1223−1225. (b) Kobayashi, K.; Sano, Y.; Nagase, S. *J. Comput. Chem.* **2001**, *22*, 1353−1358. (c) Alvarez, L.; Pichler, T.; Georgi, P.; Schwieger, T.; Peisert, H.; Dunsch, L.; Hu, Z.; Knupfer, M.; Fink, J.; Bressler, P. Mast, M.; Golden, M. S. *Phys. Rev. B* **2002**, *66*, 035107/1−035107/7.
(5) (a) Aihara, J. *Phys. Chem., Chem. Phys.* **2001**, *3*, 1427−1431. (b) Aihara, J. *Chem. Phys. Lett.* **2001**, *343*, 465−469. (c) Aihara, J. *J. Phys. Chem. A* **2002**, *106*, 11371−11374.
(6) Campanera, J. M.; Bo, C.; Poblet, J. M. *Angew. Chem., Int. Ed.* **2005**, *44*, 7230−7233.
(7) Ge, Z.; Duchamp, J. C.; Cai, T.; Gibson, H. W.; Dorn, H. C. *J. Am. Chem. Soc.* **2005**, *127*, 16292−16298.
(8) Maggini, M.; Scorrano, G.; Prato, M. *J. Am. Chem. Soc.* **1993**, *115*, 9798−9799.
(9) Cai, T.; Ge, Z.; Iezzi, E. B.; Glass, T. E.; Harich, K.; Gibson, H. W.; Dorn, H. C. *Chem. Commun.* **2005**, 3594−3596.
(10) (a) Iezzi, E. B.; Duchamp, J. C.; Harich, K.; Glass, T. E.; Lee, H. M.; Olmstead, M. M.; Balch, A. L.; Dorn, H. C. *J. Am. Chem. Soc.* **2002**, *124*, 524−525. (b) Lee, H. M.; Olmestead, M. M.; Iezzi, E.; Duchamp, J. C.; Dorn, H. C.; Balch, A. L. *J. Am. Chem. Soc.* **2002**, *124*, 3494−3495.
(11) Cardona, C. M.; Kitaygorodskiy, A.; Ortiz, A.; Herranz, M. A.; Echegoyen, L. *J. Org. Chem.* **2005**, *70*, 5092−5097
(12) Cardona, C. M.; Kitaygorodskiy, A.; Echegoyen, L. *J. Am. Chem. Soc.* **2005**, *127*, 10448−10453.

10.1021/ja0601843 CCC: $33.50

Scheme 1. 1,3-Dipolar Cycloadditon Reaction of $Sc_3N@C_{80}$ with *N*-Triphenylmethyl-5-oxazolidineone

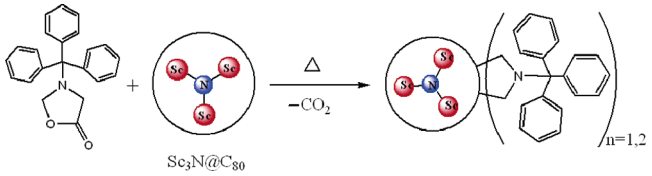

cycloaddition reaction of *N*-ethylpyrrolidino-[5,6]-$Sc_3N@C_{80}$ has also been reported.[13] Campanera et al. recently predicted that the 5,6-ring junction is the most reactive site in the case of both the free I_h C_{80} cage and the TNT-encapsulated C_{80} cage, taking into account the double bond character and the pyramidalization angle of the C−C bonds.[14]

Very recently, Asasaka and co-workers have reported the synthesis and characterization of *N*-tritylpyrrolidino adduct of the I_h isomer of $La_2@C_{80}$.[15] In that study both the 5,6- and 6,6-ring junction adduct isomers were formed, but it was the 6,6-isomer that could be separated through crystallization. Both experimental and theoretical studies suggested that the two La atoms are localized in the 6,6-adduct C_{80} cage.

In this paper we report that the addition of the *N*-tritylazomethine ylide occurs at both the 5,6- and 6,6-ring junctions of the $Sc_3N@C_{80}$ I_h cage. The two monoadducts were fully characterized by NMR spectroscopy and X-ray crystallography. A kinetic study suggests that the 6,6-ring junction adduct is the kinetically controlled product; it can interconvert into the thermodynamic product, the 5,6-ring junction adduct, at elevated temperatures. In addition, the partial characterization of the bisadducts of I_h $Sc_3N@C_{80}$ is also reported.

Results and Discussion

I. Prato Reaction on I_h $Sc_3N@C_{80}$. Reaction Kinetics and Product Isolation. A chlorobenzene solution of the pure I_h isomer of $Sc_3N@C_{80}$ and *N*-triphenylmethyl-5-oxazolidinone (in excess) was heated at reflux under nitrogen (Scheme 1). The progress of the reaction was monitored by high performance liquid chromatography (HPLC) as shown in Figure 1. After 4 h (Figure 1b), two new peaks appeared at 38.6 min (**1a**) and 43.7 min (**1b**); these are assigned as the *N*-tritylpyrrolidino monoadducts of I_h $Sc_3N@C_{80}$. Unreacted I_h $Sc_3N@C_{80}$ was later eluted at 87.8 min. **1a** and **1b** were eluted earlier than $Sc_3N@C_{80}$ because of significant differences in the polarizability and solubility caused by the trityl groups. From the HPLC trace for the 4 h reaction time (Figure 1b), the intensity of peak for **1b** is higher than that of **1a**. However, after 8 h, the amounts of product **1a** and **1b** became nearly equivalent (Figure 1c). After 12 h, the amount of **1a** exceeded that of **1b**, becoming the major product. According to the time evolution of the relative intensities of **1a** and **1b** in the HPLC traces, it appeared that **1a** was the thermodynamically stable product, but product **1b** was kinetically favored.

MALDI-TOF mass spectra of **1a** and **1b** (Figure 2a, b), under negative ionization conditions, both show strong M^- peaks at *m*/*z* 1395 and fragment peaks of the parent cage $Sc_3N@C_{80}$ at

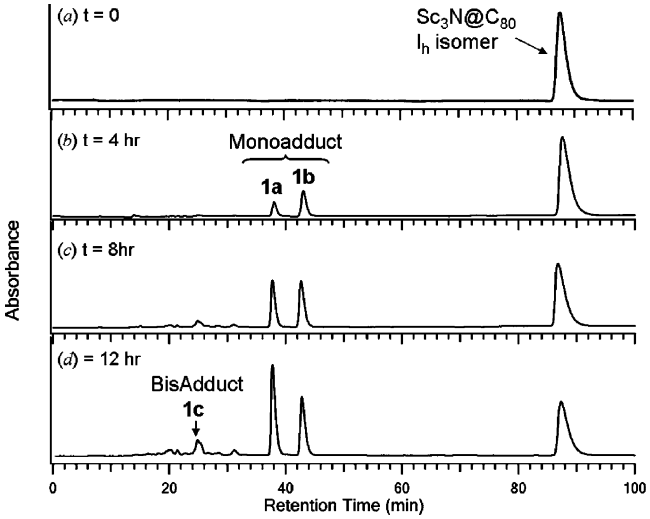

Figure 1. HPLC chromatograms of a reaction mixture for the $Sc_3N@C_{80}$ I_h isomer at times (a) 0 h, (b) 4 h, (c) 8 h, (d) 12 h. HPLC conditions: 10 mm × 250 mm PYE column at 1.0 mL min^{-1} flow rate with toluene, 390 nm detection.

m/*z* 1109. With positive ionization, MALDI-TOF mass spectra of **1a** and **1b** revealed the loss of the trityl group (Supporting Information), as expected on the basis of the high stability of the trityl cation.

A small amount of bisadduct **1c** was observed after 12 h of reaction (Figure 1d). In a fashion analogous to the MALDI-TOF mass spectrum for the first bisadduct of $Gd_3N@C_{80}$ reported by Stevenson et al.,[16] we observed a strong M^- signal at *m*/*z* 1682 for the isolated bisadduct sample **1c** (Figure 2c). The fragment peak at *m*/*z* 1438 results from the loss of the trityl group from one of the tritylpyrrolidino groups of **1c.** The fragment peak at *m*/*z* 1396 is due to complete loss of one of the tritylpyrrolidino groups. Complete loss of both tritylpyrrolidino groups (M-572) gives the $Sc_3N@C_{80}$ ion fragment peak at *m*/*z* 1110. It is worth noting that the retention time for the bisadduct is significantly shorter than those of the monoadducts, in accord with solubility and polarizability changes reflective of two exohedral trityl functional groups.

II. Structure Determination of the Products. The TNT endohedral metallofullerenes behave as 1,3-dipolarophiles and reactive 2π components in 1,3-dipolar cycloadditions with azomethine ylides. Therefore, the *N*-tritylazomethine ylide can only react with a localized double bond at one of the two types of ring junctions available on the I_h symmetric C_{80} cage. The 5,6-ring junction is abutted by two six membered rings (Figure 3A), and the 6,6-ring junction is abutted by one five- and one six-membered ring (Figure 3B). Moreover, there is statistically the same number for the two types of double bonds per molecule (60 total 5,6- and 60 6,6-ring junction bonds, respectively). The 5,6-ring junction has a horizontal plane of symmetry that leads to a tritylpyrrolidino derivative with two equivalent methylene carbons each bearing nonequivalent geminal protons in the pyrrolidine ring (Figure 3C). In contrast, since there is no horizontal symmetric plane, the 6,6-ring junction adduct has two nonequivalent methylene carbons, and the two sets of protons on these carbons are nonequivalent (Figure 3D). Because of the nonplanar nature of the pyrrolidine ring, the 6,6-isomer

(13) Martin, N.; Altable, M.; Filippone, S.; Domenech, A. M.; Echegoyen, L.; Cardona, C. M. *Angew. Chem., Int. Ed.* **2006**, *45*, 110−114.
(14) Campanera, J. M.; Bo, C.; Poblet, J. M. *J. Org. Chem.* **2006**, *71*, 46−54.
(15) Yamada, M.; Wakahara, T.; Nakahodo, T.; Tsuchiya, T.; Maeda, Y.; Akasaka, T.; Yoza, K.; Horn, E.; Mizorogi, N.; Nagase, S. *J. Am. Chem. Soc.* **2006**, *128*, 1402−1403.
(16) Stevenson, S.; Stephen, R. R.; Amos, T. M.; Cadorette, V. R.; Reid, J. E.; Phillips, J. P. *J. Am. Chem.* Soc. **2005**, *127*, 12776−12777.

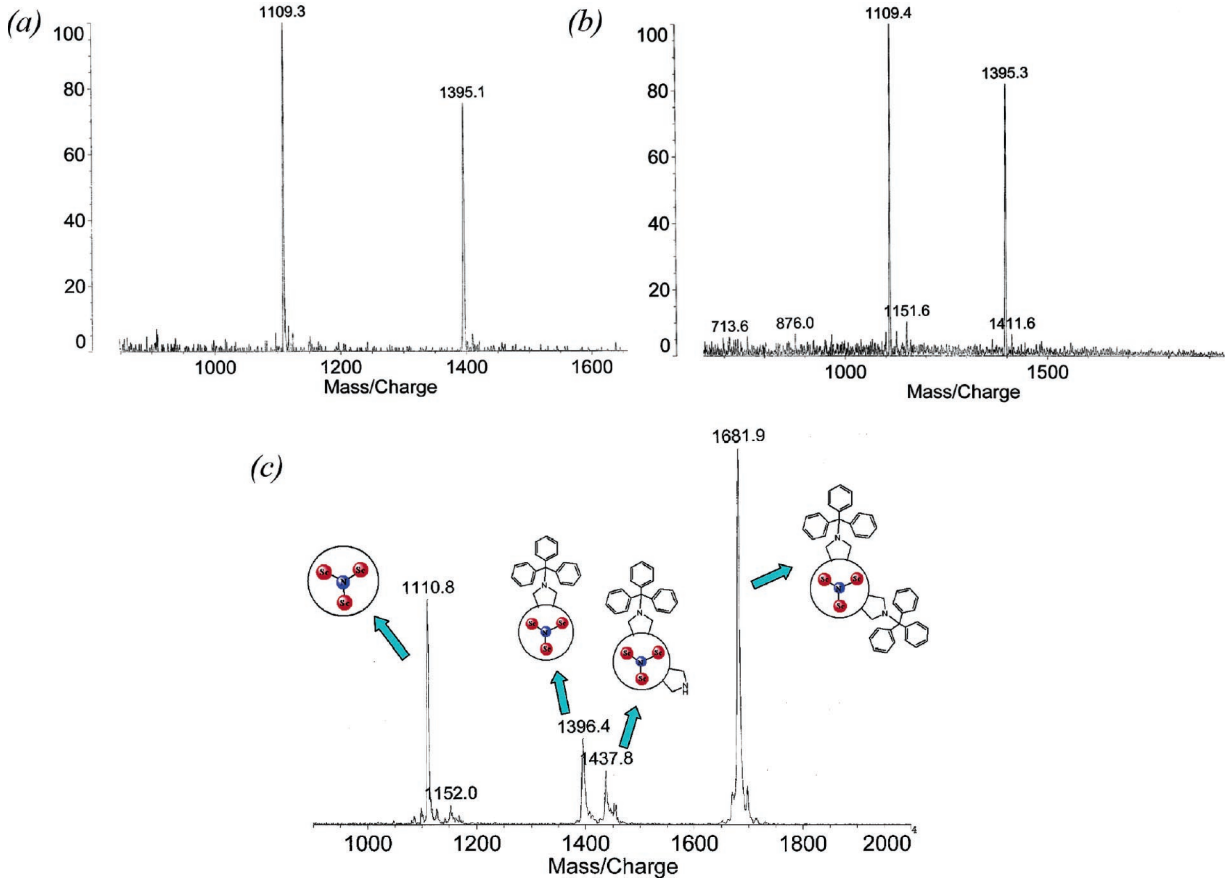

Figure 2. MALDI-TOF mass spectra using a 9-nitroanthracene matrix and negative ionization: (a) **1a**, (b) **1b**, (c) **1c**.

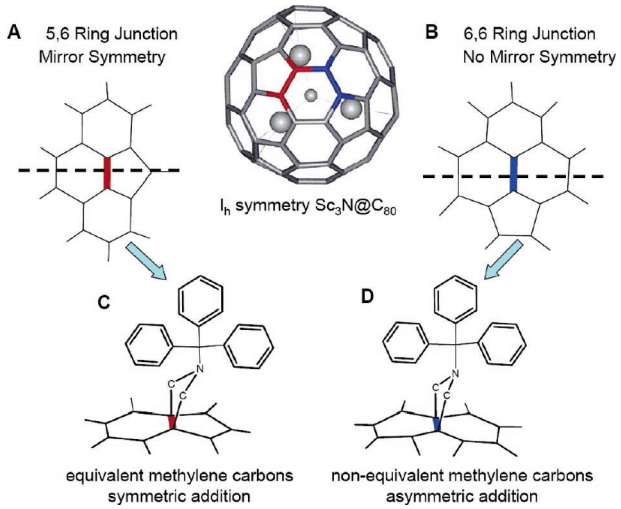

Figure 3. (A and B) Two addition sites on the $Sc_3N@C_{80}$ I_h symmetrical cage; (C) symmetric 5,6-ring junction addition model; (D) asymmetric 6,6-ring junction addition model.

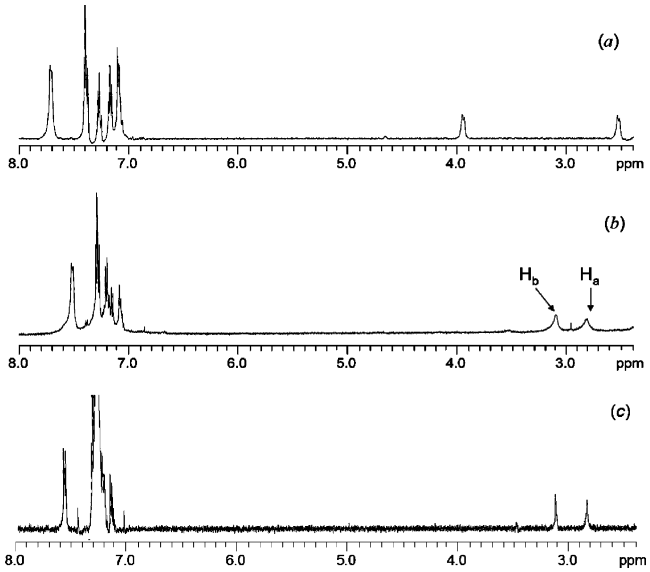

Figure 4. ^{1}H NMR spectra (500 MHz) of the $Sc_3N@C_{80}$ I_h isomer monoadducts (a) **1a** in 10:90 (v:v) CD_3COCD_3/CS_2 at 25 °C; (b) **1b** in 10:90 (v:v) CD_3COCD_3/CS_2 at 25 °C; (c) **1b** in $CDCl_3$ at 55 °C.

will exist as a pair of enantiomers that can interconvert through inversion of the pyrrolidine ring.

Monoadduct **1a** displayed ^{1}H and ^{13}C NMR (Figures 4a, 5a), COSY, and HMQC spectra (Supporting Information) analogous to those of our previously reported *N*-methyl analogue from the I_h isomer,[9] and thus we assigned **1a** the structure resulting from addition across the 5,6-ring junction, producing equivalent carbon atoms (62.6 ppm) in the pyrrolidine ring, but diastereotopic geminal protons (2.53, 3.95 ppm) in each of the methylene groups, producing an equivalent AB quartet for each pair. The NMR data of **1a** also agree with the reported assignment for the 5,6-ring junction adduct of $La_2@C_{80}$.[15]

The proton NMR spectrum of **1b** at room temperature in 10:90 CD_3COCD_3/CS_2 exhibits two broad singlets for the methylene protons at 2.82 (H_a) and 3.11 (H_b) ppm (Figure 4b), but at 55 °C in $CDCl_3$ pyrrolidine ring inversion occurs more rapidly, yielding time-averaged signals that integrate to a ~2:2 ratio (Figure 4c). The COSY spectrum (not shown) demonstrates

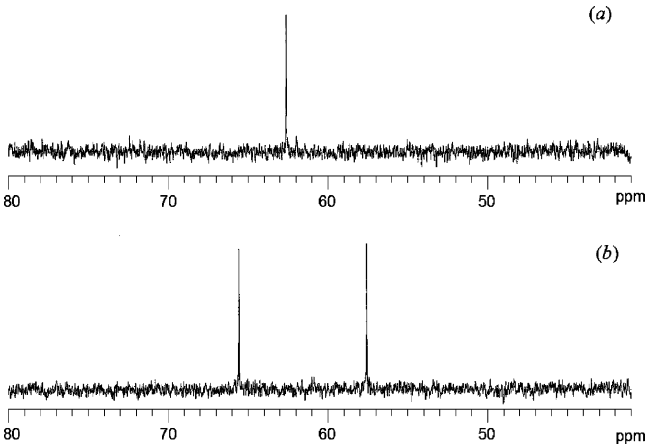

Figure 5. ^{13}C NMR spectra (125 MHz) of the $Sc_3N@C_{80}$ I_h isomer monoadducts (methylene carbons in the pyrrolidine ring ^{13}C enriched) (a) **1a** in 10:90 (v:v) CD_3COCD_3/CS_2 at 25 °C; (b) **1b** in 10:90 (v:v) CD_3COCD_3/CS_2 at 25 °C.

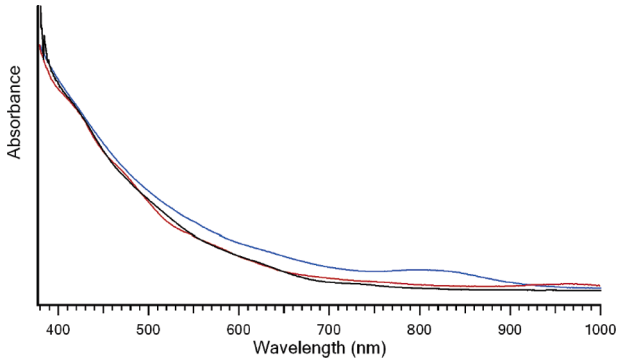

Figure 6. UV−vis spectra of $Sc_3N@C_{80}$ I_h isomer (black line), **1a** (red line) and **1b** (blue line) in CS_2 solution.

that these methylene proton signals are not coupled; therefore, the two signals are consistent with two pairs of geminal protons in nonequivalent chemical environments. The ^{13}C NMR spectrum of **1b** (with ^{13}C-enriched methylene carbons in the pyrrolidine ring by use of labeled starting material) shows two resonances of equal intensity at 65.6 and 57.6 ppm (Figure 5b). Furthermore, the HMQC spectrum (Supporting Information) reveals that the two protons are correlated to two nonequivalent carbon atoms. Thus, unlike **1a**, in which the two carbons of the pyrrolidine ring are equivalent (Figure 5a), the methylene carbons of **1b** are nonequivalent. Therefore, the addition pattern for **1b** must be asymmetric. This conclusion is consistent with the results of Echegoyen's group for the asymmetric addition of azomethine ylides on I_h $Y_3N@C_{80}$;[12] the pyrrolidine ring carbons and geminal hydrogens in this case have similar NMR shift differences but are significantly more deshielded, whereas the methylene proton signals for the 6,6-ring junction $La_2@C_{80}$ adduct show two singlet signals at 3.22 and 3.45 ppm,[15] which is quite similar to our finding for **1b**. Thus, we assign **1b** as the 6,6-ring junction adduct for the I_h isomer of $Sc_3N@C_{80}$ (Figure 3D).

The UV−vis spectrum (Figure 6) of monoadduct **1a** is similar to that of pristine I_h $Sc_3N@C_{80}$. However, it is worth noting that there is a broad spectral absorption peak centered at 800−820 nm for **1b** which is not present in **1a**. In previous studies of bisadducts and triadducts of C_{60} fulleropyrrolidines, regio-

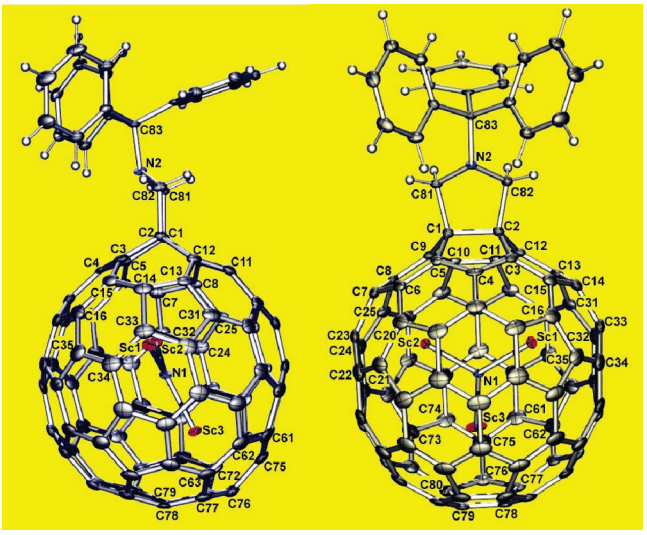

Figure 7. Two orthogonal views of the 5,6-isomer in **1a**·$2.15C_6H_6$·$0.35C_5H_{12}$ with thermal ellipsoids at 30% probability. The solvate molecules are omitted for clarity.

isomeric adducts exhibited distinct absorption patterns in the corresponding UV−vis spectra,[17,18] and this was found to be a useful tool for addition pattern assignments. Specifically, the spectra do not appear to be dependent on the nature of the addend but are characteristic of the regiochemistry for each isomer.[17] Therefore, the characteristic absorption behavior centered at 800 nm for **1b** could be associated with the regioaddition site on the I_h C_{80} cage; namely, the 6,6-adduct. In addition, the distinctive differences in the ^1H NMR spectra for **1a** and **1b** suggest that the aromaticity of the fullerene cage has been significantly altered for the 6,6-adduct when compared with the 5,6-ring junction mono-addition product.

The X-ray crystal structure of the solvate of the 5,6-isomer **1a**·$2.15C_6H_6$·$0.35C_5H_{12}$ confirms that symmetric addition has occurred at the 5,6-ring junction as shown in Figure 7. The trityl group on the pyrrolidine ring is positioned to minimize contact with the fullerene. The lone pair of electrons on the nitrogen atom in the pyrrolidine ring is located over the pentagonal ring rather than over the hexagonal ring on the C_{80} cage. As a result of adduct formation, the C1−C2 length (1.619(4) Å) at the site of addition is longer than the average C−C bond length (1.437 Å) expected for the carbon atoms in a 5,6-ring junction.[10b]

The molecule contains disordered scandium positions that fall into two Sc_3N sets, with a common nitrogen atom for each. The two sets of three scandium atoms, {Sc1, Sc2, Sc3} and {Sc4, Sc5, Sc6} refined to occupancies of 0.90(3) and 0.10(7), respectively. The major Sc_3N set is planar with the sum of the three Sc−N−Sc angles equaling 359.79°; the minor set is similar with the sum of the other three Sc−N−Sc angles equaling 357.9°. Figure 7 shows only the location of the major set. The orientation of the major planar Sc_3N unit is surprisingly similar to that of the previously reported Diels−Alder adduct in which the internal cluster is positioned well away from the external functionalization site.[10] The dihedral angle of the planes of the Sc_3N cluster and the pyrrolidino ring ($C_1-C_2-C_{81}-C_{82}$) is

(17) (a) Kordatos, K.; Bosi, S.; Da Ros, T.; Zambon, A.; Lucchini, V.; Prato, M. *J. Org. Chem.* **2001**, *66*, 2802−2808. (b) Ishi-i, T.; Nakashima, K.; Shinkai, S. *Chem. Commun.* **1998**, 1047−1048. (c) Taki, M.; Sugita, S.; Nakamura, Y.; Kasashima, E.; Yashima, E.; Okamoto, Y.; Nishimura, J. *J. Am. Chem. Soc.* **1997**, *119*, 926−932.
(18) Marchesan, S.; Ros, T. D.; Prato, M. *J. Org. Chem.* **2005**, *70*, 4706−4713.

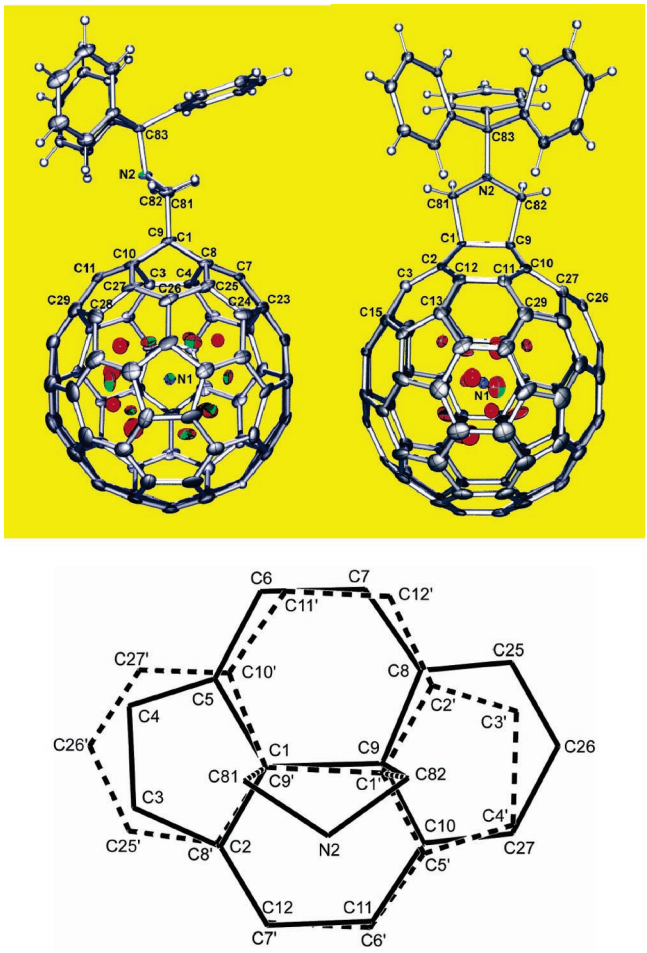

Figure 8. (Top) Two orthogonal views of the 6,6-isomer in **1b**·2.25CS_2·0.75C_6H_6 showing the position of the major cage site (with 0.75 occupancy) with thermal ellipsoids at 30% probability. The positions of the 15 sites containing scandium ions with fractional occupancies ranging from 0.40 to 0.06 are shown in red. (Bottom) Drawing of a portion of the fullerene cage **1b** showing the orientation of the minor form, shown with dashed lines, relative to the major form, shown with solid lines.

26.35°, which is very close to that in the Diels−Alder adduct (27.06°). The N−Sc distances in the major form [2.031(2), 2.030(3), and 2.029(2) Å] are also very comparable to those in the Diels−Alder adduct [2.032(3), 2.020(3), and 2.029(3) Å].[10]

Similarly, the X-ray crystal structure of the solvate **1b**·2.25CS_2·0.75C_6H_6 confirms that addition has occurred at a 6,6-ring junction. Figure 8 shows drawings of the structure as determined crystallographically. The two orthogonal views of one enantiomer of the major form are shown at the top of Figure 8. Since the compound crystallizes in the centrosymmetric space group $P\bar{1}$, the other enantiomer is present and generated by symmetry. There is disorder in the cage location. Only the major form, which has 0.75 occupancy, is shown in the two views at the top of Figure 8. In addition to the orientation shown in the two views at the top of Figure 8, there is a second orientation of the fullerene cage that interchanges the positions of the five- and six-membered rings that radiate from the sites of addition. This situation arises because the two enantiomers of the 6,6-isomer crystallize in unequal amounts at a common site. A line drawing showing a portion of both orientations (enantiomers) superimposed is shown in the lower part of Figure 8. Note that this disorder does not jeopardize the conclusion that addition has occurred at a 6,6-ring junction. As a result of adduct formation the C1−C9 bond length (1.619(7) Å) is longer than the average C−C bond length (1.421 Å) at an unfunctionalized 6,6-ring junction.[10b]

There is also disorder in the interior of the C_{80} that involves the locations of the scandium atoms. There are 10 scandium atom sites with site occupation factors (SOFs) ranging from 0.187 to 0.398. These were refined with anisotropic thermal parameters. There are five additional scandium atom sites with SOFs ranging from 0.065 to 0.097, and these were assigned isotropic thermal parameters. The occupancies of these scandium positions were independently varied but were constrained to sum to 3.00000. No clear correlation between the occupancies of these 15 sites could be discerned. All 15 sites are shown in Figure 8. Notice, however, that none of these scandium atom sites is near the site of external adduct formation. The presence of 15 sites for scandium atoms within this endohedral is consistent with earlier calculations that show little energetic differences between varying orientations of the Sc_3N group within the I_h isomer of unfunctionalized C_{80}.[19] The structure also contains disorder in the solvate CS_2 and benzene molecules, which are not shown in the figure. The structure of the fullerene cage and the appended group of the tritylpyrrolidino 6,6-adduct of $La_2@C_{80}$ is similar to that of the 6,6-isomer **1b** reported here.[15] That adduct also crystallized as a racemate in the space group $P\bar{1}$.

III. Interconversion of Isomeric Prato Monoadducts 1a and 1b. To demonstrate that the 6,6-adduct **1b** is indeed the kinetic product and the 5,6-adduct **1a** is the thermodynamic product we carried out an interconversion study. A chlorobenzene solution of pure 6,6-junction adduct **1b**, the purported kinetic product, was heated at reflux for 2 days; the composition of the solution was monitored via HPLC. The results of this study are shown in Figures 9 and 10. Over time, the 6,6-adduct **1b** is converted to >90% 5,6-adduct **1a**, the thermodynamically more stable isomer. The half-life for this process is 11.5 h (at ∼130 °C).

Mechanistically the interconversion of the isomers of the monoadducts **1a** and **1b** is an interesting process. Although such equilibrations have been reported for C_{60} derivatives,[20] to our knowledge, this is the first such isomerization process to be observed for an endohedral metallofullerene. Based on the principle of microscopic reversibility,[21] the expected mechanism for this process involves the same intermediate that is presumed to be involved in the initial formation of **1b**, i.e., the zwitterionic species resulting from initial attack of the azomethine ylide, which has a negative charge on the C_{80} cage and a positive charge on the azomethine ylide moiety (Figure 11, middle). After rotation about the CH_2−C_{80} bond, bond formation at the 5,6-ring juncture would then yield the thermodynamic product **1a** (Figure 11). We are currently investigating the activation

(19) Campanera, J. M.; Bo, C.; Olmstead, M. M.; Balch, A. L.; Poblet, J. M. *J. Phys. Chem. A* **2002**, *106*, 12356−12364.
(20) Huang, S.; Xiao, Z.; Wang, F.; Zhou, J.; Yuan, G.; Zhang, S.; Chen, Z.; Thiel, W.; Schleyer, P.; Zhang, X.; Hu, X.; Chen, B.; Gan, L. *Chem. Eur. J.* **2005**, *11*, 5449−5456.
(21) Tolman, R. *Proc. Natl. Acad. Sci., U.S.A.* **1937**, *11*, 436−439. Tolman, R. C. *The Principles of Statistical Mechanics*; Oxford University Press: London, UK, 1938. Gould, E. S. *Mechanism and Structure in Organic Chemistry*; Henry Holt and Co.: New York, 1959; p 319. Jackson, W. G. *Inorg. Chem.* **1987**, *26*, 3004−3007. Chandrasekhar, S. *Res. Chem. Intermed.* **1992**, *17*, 173−209. Saveant, J.-M. *J. Electroanal. Chem.* **2000**, *485*, 86−88.

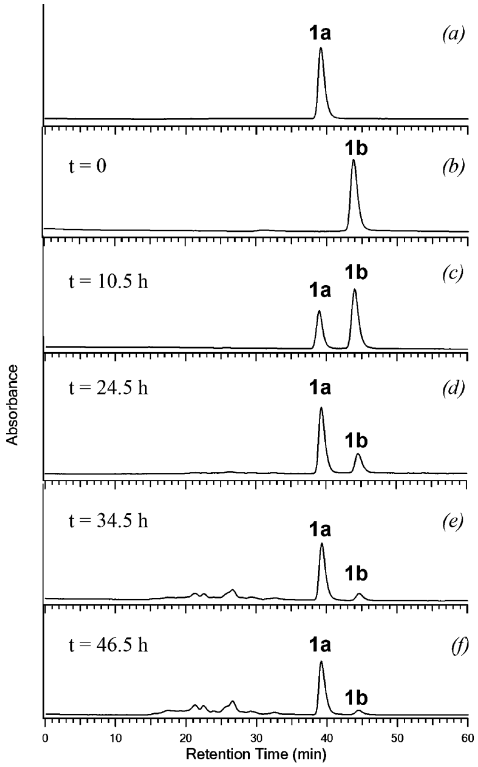

Figure 9. HPLC chromatograms of interconversion of **1b** to **1a**, (a) pure **1a**, (b) $t = 0$ h, pure **1b**, (c) $t = 10.5$ h, (d) $t = 24.5$ h, (e) $t = 34.5$ h, (f) $t = 46.5$ h.

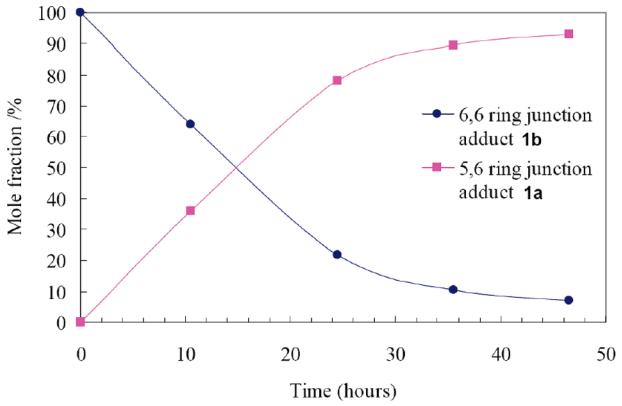

Figure 10. The change of composition of **1b** and **1a** during the interconversion process.

energy for the interconversion process along with detailed computational studies which will be reported separately.

Conclusions

Both the kinetically and thermodynamically controlled *N*-tritylpyrrolidino derivatives of I_h $Sc_3N@C_{80}$ have been synthesized and isolated. Kinetic studies clearly demonstrate that the 5,6-ring junction adduct (**1a**) is the thermodynamic product, whereas the 6,6-ring junction adduct (**1b**) is the kinetic product. The structures of the 5,6- and 6,6-adducts were confirmed by X-ray crystallography. The kinetic product **1b** was converted to the thermodynamic product **1a** in refluxing chlorobenzene at 130 °C. By acid-catalyzed removal of the trityl protecting group, these *N*-tritylpyrrolidino derivatives promise to be useful precursors for various applications as shown with C_{60} analogues.[22]

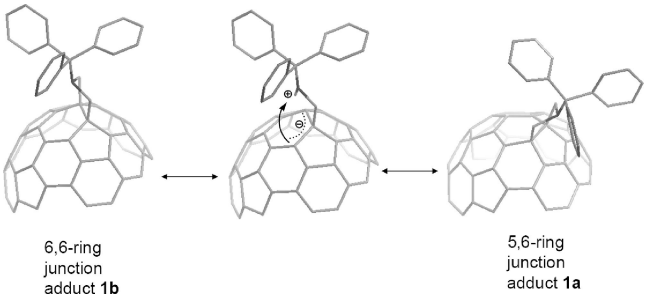

Figure 11. Proposed mechanism of interconversion of **1b** to **1a** through the pirouette of the addend.

Experimental Section

Materials and Methods. The $Sc_3N@C_{80}$ I_h and D_{5h} isomer mixture was obtained by the chemical separation method, as reported in detail earlier.[7] *N*-Triphenylmethyl-5-oxazolidinone was synthesized according to previous work.[8] Formaldehyde (99% ^{13}C, ~20% w/w in H_2O, Cambridge Isotope Laboratory, Inc.) was used for synthesizing ^{13}C enriched *N*-triphenylmethyl-5-oxazolidinone. Toluene (HPLC grade ≥ 99.9%) and chlorobenzene (99%) were used as obtained from Aldrich. A semi-preparative PYE [β-(1-pyrenyl)ethyl silica] column (10 mm × 250 mm) and a guard PYE column (10 mm × 20 mm) were used for both analysis and purification. HPLC system: Acure series III pump, 757 absorbance detector (Applied Biosystems). A JEOL ECP 500 MHz instrument was used for all NMR measurements. Mass spectrometry was performed on a Kratos Analytical Kompact SEQ MALDI-TOF mass spectrometer. Samples were dissolved in carbon disulfide and 0.5 μL of solution was placed on the stainless steel target plates. An equal volume of saturated solution of the 9-nitroanthracene matrix in toluene was added, and the mixture was evaporated to dryness. Analysis was performed in the typical manner, whereby the dried sample on the target plate was subjected to irradiation from a nitrogen laser (227 nm), and the resulting ions formed were detected and recorded. The accelerating voltage applied was 20 kV. Minimal laser power was used to achieve sufficient sensitivity, while avoiding degradation of the signal in terms of resolution and noise.

Purification of Isomeric $Sc_3N@C_{80}$. The $Sc_3N@C_{80}$ I_h and D_{5h} isomer mixture was dissolved in toluene. Pure $Sc_3N@C_{80}$ I_h isomer was isolated from the original mixture by HPLC using a PYE column, with toluene @ 1.0 mL/min, $\lambda = 390$ nm.

Reaction of I_h Isomer of $Sc_3N@C_{80}$ with *N*-Trityloxazolidinone. A solution of 2.0 mg (1.8 μmol) of $Sc_3N@C_{80}$ I_h isomer and 30 mg (91 μmol) of *N*-triphenylmethyl-5-oxazolidinone in 35 mL of chlorobenzene was heated at reflux under nitrogen. The solvent was removed by a rotary evaporator. The residue was dissolved in toluene and then injected into an HPLC for analysis. **1a**, **1b**, and **1c** were isolated by HPLC using the same conditions as indicated above.

X-ray Crystallographic Analysis of the 5,6-Isomer 1a. Black needles of the 5,6-isomer **1a**·$2.15C_6H_6$·$0.35C_5H_{12}$ were crystallized from benzene/pentane by slow vapor diffusion of the latter at room temperature. The crystals were removed from the glass tubes, in which they were grown, together with a small amount of mother liquor and immediately coated with a hydrocarbon oil on a microscope slide. A suitable crystal was mounted on a glass fiber with silicone grease and placed in the cold dinitrogen stream of a Bruker Apex II CCD with graphite-monochromated Mo Kα radiation at 90(2) K. No decay was observed in 50 duplicate frames at the end of each data collection. Crystal data are given below. The structures were solved by direct methods and refined using all data (based on F^2) using the software of

(22) Prato, M.; Maggini, M.; Giacometti, C.; Scorrano, G.; Sandona, G.; Farnia, G. *Tetrahedron* **1996**, *52*, 5221−5234. Kurz, A.; Halliwell, C. M.; Davis, J. J.; Hill, H. A. O.; Canters, G. W. *Chem. Commun.* **1998**, 433−434. Capaccio, M.; Gavalas, V. G.; Meier, M. S.; Anthony, J. E.; Bachas, L. G. *Bioconjugate Chem.* **2005**, *16*, 241−244.

SHELXTL 5.1.[23] A semiempirical method utilizing equivalents was employed to correct for absorption.[24] Hydrogen atoms were added geometrically and refined with a riding model.

The molecule contains disordered scandium atoms that can be assigned to two Sc_3N sets, with a common nitrogen atom in each. The two sets of three scandium atoms, {Sc1, Sc2, Sc3} and {Sc4, Sc5, Sc6} refined to set occupancies of 0.90(3) and 0.10(7), respectively. The structure contains a region of disordered solvent that was modeled with three-half-occupied molecules of benzene and a molecule of *n*-pentane at 0.35 fractional occupancy. These molecules were refined as rigid groups. In addition, there is a molecule of benzene located on a position of inversion symmetry.

Crystal data for the 5,6-isomer 1a·2.15C_6H_6·0.35C_5H_{12}: black needles, $C_{115.65}H_{36.10}N_2Sc_3$; crystal size 0.24 × 0.09 × 0.013 mm; triclinic; space group $P\bar{1}$; a = 11.0242(11) Å, b = 16.5046(18) Å, c = 18.8995(19) α = 74.045(2)°, β = 77.655(3)°, γ = 76.840(2)°, V = 3177.2(6) Å^3, Z = 2, d_{calcd} = 1.660 Mg/m^3, F(000) = 1614, λ(Mo Kα) = 0.71073 Å, μ(Mo Kα) = 0.382 mm^{-1}, θ range for data collection 1.92−25.68°, T = 90(2) K; reflections collected 31897, independent reflections 12063 [R(int) = 0.0407], Completeness to θ = 25.68°, 99.9%, Refinement method: full-matrix least squares on F^2; data/restraints/parameters: 12063/0/1066; Goodness-of-fit on F^2 1.029; Final R indices [$I > 2\sigma(I)$]: R1 = 0.0817, wR2 = 0.1390; R indices (all data): R1 = 0.0817, wR2 = 0.1559; Largest diff. peak and hole: 1.141 and −0.679 e·Å^{-3}.

X-ray Crystallographic Analysis of the 6,6-Isomer 1b. Black plates of the 6,6-isomer **1b**·2.25CS_2·0.75C_6H_6 were formed by layering 0.5 mL of benzene over a solution of 2−5 mg of **1b** in 0.5 mL of carbon disulfide in a 6-mm inside diameter glass tube. Methanol (0.5 mL) was layered over the benzene layer, and the tube was capped with a permeable rubber septum. Crystals grew in 1−2 weeks. Crystals were harvested and data collected as described above for the 5,6-isomer **1a**. The structure contains disorder in the solvate CS_2 and benzene molecules.

Crystal data for the 6,6-isomer 1b·2.25CS_2·0.75C_6H_6: black plates, $C_{107.75}H_{23.50}N_2S_{4.50}Sc_3$; crystal size 0.24 × 0.11 × 0.016 mm; triclinic; space group $P\bar{1}$; a = 11.0127(8) Å, b = 16.3870(8) Å, c = 18.7355(11) Å, α = 99.521(1)°, β = 106.034(1)°, γ = 102.488(1)°, V = 3080.0(3) Å^3, Z = 2, d_{calcd} = 1.752 Mg/m^3, F(000) = 1638, λ = 0.71073 Å, μ(Mo Kα) = 0.543 mm^{-1}, θ range for data collection 1.95−27.50°, T = 90(2) K; reflections collected 35232; independent reflections 14160 [R(int) = 0.0445], completeness to θ = 27.50°, 99.9%, refinement method: full-matrix least-squares on F^2; data/restraints/parameters: 14160/463/1214; goodness-of-fit on F^2 1.104; final R indices [$I > 2\sigma(I)$]: R1 = 0.099, wR2 = 0.281; R indices (all data): R1 = 0.141, wR2 = 0.30525; largest diff. peak and hole: 1.819 and −1.509 e.Å^{-3}.

Acknowledgment. We are grateful for support of this work by the National Science Foundation [CHE-0437300 (H.C.D.), DMR-0507083 (H.C.D., H.W.G.), and CHE 0413857 (A.L.B.)].

Supporting Information Available: COSY, HMQC of **1a** and **1b**; X-ray crystallographic files in CIF format for **1a**·2.15C_6H_6·0.35C_5H_{12} and for **1b**·2.25CS_2·0.75C_6H_6 This material is available free of charge via the Internet at http://pubs.acs.org.

JA0601843

(23) Sheldrick, G. M. *SHELXTL NT*, ver. 6.12; Bruker Analytical X-ray Systems, Inc.: Madison, WI, 2001.
(24) *SADABS* 2.10, Sheldrick, G. M. based on a method of Blessing, R. H. *Acta Crystallogr.: Sect. A* **1995**, *A51*, 33.